

fit to the observed data is also shown. The regression yields a correlation coefficient between Al and silica of 0.90. This correlation suggests that the concentration of dissolved Al in the water column is controlled by the same mechanism that controls dissolved silica.

Several investigators (3, 10) concluded that the distribution and concentration of dissolved silica in the oceans are regulated by the biological activity of diatoms. Our profile of dissolved Al and its covariance with dissolved silica observed in the Mediterranean Sea support the hypothesis that there is a link between the Si and Al cycles in the oceans through the activity of diatoms. The coupling of the cycles of Al and Si within the oceans through the activity of diatoms implies that the Al cycle is very similar to the Si cycle established by Wollast (10). If we assume that the Al/Si ratio in diatom frustules is approximately 0.001 (11) and the average concentration of dissolved Al in river waters is 25 $\mu\text{g/liter}$ (12), then a cycle for Al in the oceans, completely analogous to that for Si, can be constructed (Fig. 4). This cycle may maintain the oceans at steady state with respect to dissolved Al. Furthermore, Fig. 3 gives an average Al/Si ratio in seawater near Corsica of about 0.008. This is within the range of values observed for Al and Si in diatom frustules (11).

FRED T. MACKENZIE

MARC STOFFYN

Department of Geological Sciences,
Northwestern University,
Evanston, Illinois 60201

ROLAND WOLLAST

Service Environment, University of
Brussels, Brussels 1050, Belgium

References and Notes

1. L. G. Sillén, in *Oceanography*, M. Sears, Ed. (AAAS, Washington, D.C., 1961), p. 549.
2. H. D. Holland, *Proc. Natl. Acad. Sci. U.S.A.* **53**, 1173 (1965); F. T. Mackenzie and R. M. Garrels, *Am. J. Sci.* **264**, 507 (1966); R. Siever, *Sedimentology* **11**, 5 (1968); F. T. Mackenzie, in *Chemical Oceanography*, J. P. Riley and G. Skirrow, Eds. (Academic Press, New York, ed. 2, 1975), vol. 1, p. 309.
3. W. W. Broecker, *Quat. Res. (N.Y.)* **1**, 188 (1971).
4. M. Stoffyn, thesis, University of Brussels (1975).
5. A. J. van Bennekom and S. J. van der Gaast, *Geochim. Cosmochim. Acta* **40**, 1149 (1976).
6. See also J. C. Lewin, *ibid.* **21**, 182 (1961).
7. T. Shigematsu, Y. Nishikawa, K. Hiraki, N. Nagano, *Bunseki Kagaku* **19**, 551 (1970). This method measures only dissolved Al because particulate Al will not react with the chelating agent.
8. S. Caschetto analyzed the Al in the frozen samples.
9. W. M. Sackett and G. O. S. Arrhenius, *Geochim. Cosmochim. Acta* **26**, 955 (1962); J. J. Alberts, D. F. Leyden, T. A. Paterson, *Mar. Chem.* **4**, 51 (1976).
10. R. Wollast, in *The Sea*, E. D. Goldberg, Ed. (Wiley, New York, 1975), vol. 5, p. 359.
11. J. H. Martin and G. A. Knauer, *Geochim. Cosmochim. Acta* **37**, 1639 (1973); D. C. Hurd, *ibid.*, p. 2257.
12. Measurements of dissolved Al in river waters are suspect because of particulate contamination [see, for example, discussions by W. H.

Durum and J. Haffty, *ibid.* **27**, 1 (1963); V. C. Kennedy, G. W. Zellweger, B. F. Jones, *Water Resour. Res.* **10**, 785 (1974)]. Our estimate for the average dissolved Al concentration of the world's rivers is based on the following recent work: (i) B. F. Jones, V. C. Kennedy, and G. W. Zellweger [*Water Resour. Res.* **10**, 791 (1974)] reported that waters from small streams in California, after filtration through 0.1- μm filters and extraction with oxine, showed Al concentrations of 1 to 10 $\mu\text{g/liter}$. (ii) D. J. Hyde [thesis, University of East Anglia (1974)], using the

fluorometric method for Al (7), observed Al concentrations of 5 to 42 $\mu\text{g/liter}$ in waters of the Conway, Ouse, and Yare rivers, North Wales. (iii) M. Stoffyn (4), using the fluorometric method for Al (7), observed 17 $\mu\text{g/liter}$ in the Scheldt River, Belgium.

13. We thank R. M. Garrels for a critical review of this report and S. Caschetto for the analysis of the Al in the frozen samples. Supported by NSF grant EAR 76-12279.

20 September 1977

1400-Million-Year-Old Shale-Facies Microbiota from the Lower Belt Supergroup, Montana

Abstract. Carbonaceous shales of the Middle Proterozoic Newland Limestone, Belt Supergroup, Little Belt Mountains, Montana, contain abundant and well-preserved filamentous and spheroidal microfossils. The filamentous forms, ranging from less than 1 to 12 micrometers in width, are interpreted as representing the preserved sheaths of at least four species of nostocalean cyanophytes. The spheroidal forms, ranging from 15 to 108 micrometers in size, are evidently planktonic forms and are tentatively interpreted as representing the encystment stage of eukaryotic algae. The Newland microbiota is adaptable to petrographic thin-section work, and useful for evaluating the potential of such microfossils for intercontinental biostratigraphic correlation. It is the oldest shale-facies microbiota presently known from North America.

During the past 15 years, knowledge of Precambrian life has advanced rapidly with the discovery of more than 30 well-preserved microfossil assemblages (1-3). Most of the Precambrian microbiotas studied in North America occur in stromatolitic cherts; the constituent micro-

fossils largely represent shallow-water, benthic mat communities (2). Such communities may not embrace the entire spectrum of Precambrian life (2, 4-6). Furthermore, some of these microbiotas

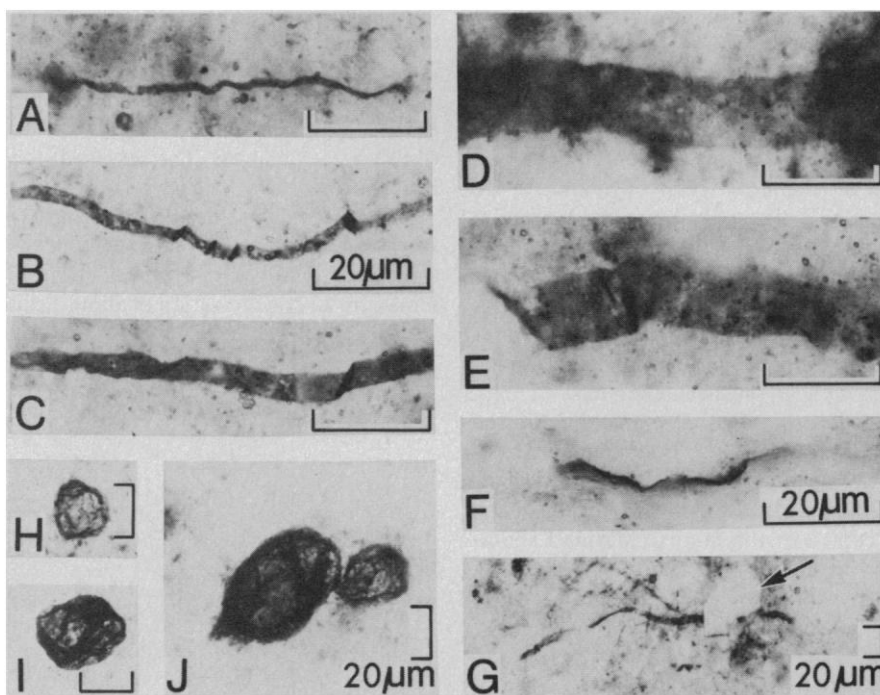


Fig. 1. Optical photomicrographs (transmitted light) of microfossils in petrographic thin sections of carbonaceous shales from the Newland Limestone, Little Belt Mountains, Montana. All thin sections, except (F), are oriented parallel to bedding; (F) is oriented perpendicular to bedding. Small-diameter filaments (A to C, F, and G), large-diameter filaments (D and E), and spheroids (H to J) are shown. Filaments shown in (C) and (F) are of comparable dimension and degree of preservation but are viewed in different orientations [(C) is viewed in a thin section ground parallel to bedding; (F) in a section ground perpendicular to bedding]. In (G), a diagenetic feldspar grain (arrow) is shown disrupting a filament. Bar for scale is 20 μm in each photomicrograph.

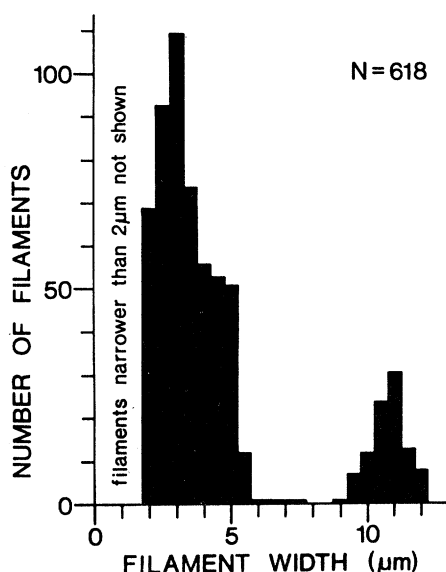


Fig. 2. Size range of filamentous microfossils measured in shales from the Newland Limestone (44 cm² was scanned in six thin sections oriented parallel to bedding).

were apparently preserved by encasement in primary amorphous silica (7) and thus may have been further restricted by an anomalous chemical environment (2). Precambrian microfossils are known from lithologies other than stromatolitic cherts. They have been described from calcareous stromatolites (8); however, they typically are poorly preserved in such rocks because the organic material was disrupted during diagenetic recrystallization of the carbonate minerals. Microfossils have also been studied in Precambrian shales. The majority of such investigations were conducted in the Soviet Union (9) and in western Europe (6). Shale facies provide an opportunity to sample planktonic organisms which may not be as environmentally restricted as the benthic mat, chert-facies microbiotas which provide most of our current understanding of Precambrian life (6, 10, 11). Moreover, shale-facies microfossils have potential value for biostratigraphic correlation of Proterozoic sedimentary sequences (6, 9). Except for carbonaceous films and compressions occurring in the 1300-million-year-old Greyson Shale (5), well-preserved microbiotas thus far described from North American shales (11, 12) are all of Late Proterozoic age (less than 900 million years old).

The shale-facies microbiota reported here was obtained from black shales of the approximately 1400-million-year-old (13) Newland Limestone of the Belt Supergroup (14) from a road cut along U.S. Highway 89 about 7 km southeast of Neihart, Montana. Acid macerations were prepared with standard palynological techniques (15); optical microscopy

of water mounts revealed the presence of numerous organic filaments measuring a few micrometers in diameter and of relatively rare organic spheroids measuring several tens of micrometers in diameter. Because of limitations inherent in the study of such macerations, however, these initial observations proved neither whether the detected microstructures were indigenous to the shale nor whether they were syngenetic with deposition of the shale. Petrographic thin sections of the shale, 20 to 50 μm thick and oriented either parallel or perpendicular to bedding, were prepared for this purpose. Microfossils were found to be abundant in several thin sections; transmitted light oil immersion optical microscopy revealed that the microfossils (i) are entirely enclosed by the argillaceous matrix of the shale; (ii) are brown in color and are not birefringent under cross-polarized light; (iii) are compressed parallel to the lamination (Fig. 1F), evidently as a result of postdepositional compaction of the argillaceous sediment; and (iv) are disrupted by diagenetic feldspar crystals (Fig. 1G). These observations indicate that the microfossils are both indigenous to the shale and syngenetic with deposition of the mineral matrix.

The filamentous forms (Fig. 1, A to G), the most abundant component of this assemblage, are apparently unbranched, initially cylindrical structures that were compressed during compaction of the surrounding argillaceous sediment. They range from less than 1 μm to 12 μm in width (Fig. 2), lack cross walls or other evidence of cellular organization (16), are oriented parallel to bedding, and occur as both isolated filaments and fragments of filament mats. They are interpreted as representing the preserved sheaths of at least four species of nostocalean cyanophytes (17).

The spheroidal forms (Fig. 1, H to J) are smooth-walled, nongranular, unornamented, single-layered structures which resemble the sphaeromorph *Kildinella* Timofeev, 1964 (9). Thirty-seven specimens identified in petrographic thin sections range from 15 to 60 μm in size (Fig. 3); the largest specimen observed in acid maceration residue measures 108 by 68 μm. The taxonomic affinity of these spheroidal forms is not well established. The larger spheroids are significantly larger than most modern coccoid cyanophytes (3, 18) and the absence of any indication of inner sheath material suggests that they do not represent the common sheath of a colonial coccoid cyanophyte (19). A plausible interpretation, based on comparison with Phanerozoic microfossils (20), is that the larger

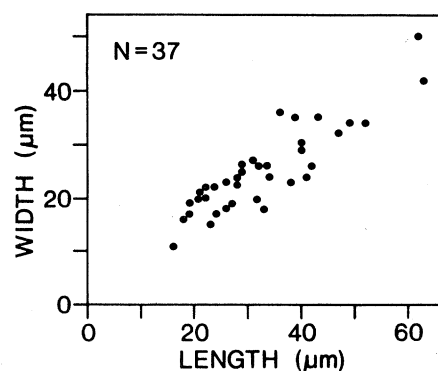


Fig. 3. Scatter diagram showing the size range of spheroidal microfossils measured in shales from the Newland Limestone (132 cm² was scanned in 15 thin sections oriented parallel to bedding).

spheroids represent the encystment stage of eukaryotic algae (5, 21).

The Newland Shale microfossils are of interest for the following reasons: (i) they represent, at least in part, a planktonic assemblage and thus add to our knowledge of Middle Proterozoic life because such organisms are not commonly represented in the more frequently studied benthic mat, chert-facies microbiotas (2, 4-6, 10, 11); (ii) the spheroidal microfossils resemble Soviet and European shale-facies microfossils of a type considered useful for biostratigraphic correlation, thus providing the opportunity to further delineate the usefulness of such microfossils for intercontinental biostratigraphic correlation of Proterozoic sedimentary sequences (6, 9); (iii) the larger spheroids may have eukaryotic affinities; (iv) they illustrate the feasibility of studying shale-facies microfossils directly in petrographic thin section (22); and (v) they are the oldest (about 1.4×10^9 years old) shale-facies microbiota presently known from North America.

ROBERT J. HORODYSKI

Department of Earth Sciences,
University of Notre Dame,
Notre Dame, Indiana 46556

BONNIE BLOESER

Department of Earth and Space
Sciences, University of California,
Los Angeles 90024

References and Notes

1. For a review of the status of Precambrian paleontology, see (2) and (3).
2. J. W. Schopf, *Annu. Rev. Earth Planet. Sci.* **3**, 213 (1975).
3. J. W. Schopf, *Origins Life* **5**, 119 (1974).
4. This is well illustrated by M. R. Walter *et al.* (5). Also see J. W. Schopf, *Biol. Rev.* **45**, 319 (1970) and (6).
5. M. R. Walter, J. H. Oehler, D. Z. Oehler, *J. Paleontol.* **50**, 872 (1976).
6. G. Vidal, *Fossils and Strata* **9**, 1 (1976).
7. J. W. Schopf, *J. Paleontol.* **42**, 651 (1968); J. W. Schopf, J. M. Blacic, *ibid.* **45**, 925 (1971); H. J. Hofmann, *ibid.* **50**, 1040 (1976).
8. L. A. Nagy, *Science* **183**, 514 (1974); R. J. Horodyski, *Precambrian Research* **2**, 215 (1975).
9. B. V. Timofeev, *Micropalaeophytological Re-*

- search into *Ancient Strata* (British Library Lending Division, Yorks, England, transl. 1974); *Plant Microfossils of the Proterozoic and Lower Paleozoic of the U.S.S.R.* (Nauka, Leningrad, 1974).
10. J. W. Schopf et al., *Precambrian Research* **4**, 269 (1977).
 11. B. Bloeser, J. W. Schopf, R. J. Horodyski, W. J. Breed, *Science* **195**, 676 (1977).
 12. Precambrian shale-facies microbios from North America have been described from the Windermere Supergroup [G. Licari and P. E. Cloud, *Geol. Soc. Am. Program 1968 Annu. Meet.* (1968), p. 174; M. Moorman, *J. Paleontol.* **48**, 524 (1974); P. E. Cloud, M. Moorman, D. Pierce, *Q. Rev. Biol.* **50**, 131 (1975); B. J. Javor and E. W. Mountjoy, *Geology* **4**, 111 (1976); H. J. Hofmann, *Geol. Surv. Canada Bull.* **189** (1971); W. C. Gussow, *J. Paleontol.* **47**, 1108 (1973)], the Chuar Group [C. D. Walcott, *Geol. Soc. Am. Bull.* **10**, 199 (1899); T. D. Ford and W. J. Breed, *Palaeontology* **16**, 535 (1973); C. Downie, in *Geology and Natural History of Grand Canyon Region, Guidebook to the Fifth Field Conference*, D. L. Baars, Ed. (Four Corners Geological Society, Flagstaff, 1969), p. 114; (11)]; the Tindir Group [C. W. Allison and M. A. Moorman, *Geology* **1**, 65 (1973)], and the Uinta Mountain Group [H. J. Hofmann, *Precambrian Research* **4**, 1 (1977)].
 13. Radiometric dates and correlation for the Belt Supergroup are reviewed by J. E. Harrison, *Geol. Soc. Am. Bull.* **83**, 1215 (1972).
 14. This area has been recently mapped by W. T. Keefer, *U.S. Geol. Surv. Misc. Geol. Invest. Map I-726* (1972).
 15. Shale samples were dissolved in hydrofluoric acid followed by centrifuging and washing the organic residue with distilled water.
 16. The dark transverse lines shown in Figs. 1, B, C, and F, are folds in the filament.
 17. Separation of the filaments into at least four species is based on the comparison of size and frequency distribution of filaments in six different laminae. These species have average apparent widths of about 11, 5, 3, and 1.5 μm . In addition, filaments as wide as 40 μm and of uncertain biologic affinity are of very rare occurrence in the Newland shales. Preferential preservation of sheaths as compared to trichomes in the oscillatoriacean cyanophyte *Lyngbya aestuarii* is illustrated by R. J. Horodyski, B. Bloeser, S. Vonder Haar, *J. Sediment. Petrol.* **47**, 680 (1977). A detailed taxonomic treatment of the Newland microfossils and of similar microfossils occurring in the underlying Chamberlain Shale is in preparation (R. J. Horodyski and B. Bloeser, in preparation.)
 18. J. W. Schopf, D. Z. Oehler, *Science* **193**, 47 (1976); P. Cloud, *Geol. Soc. S. Afr. Alex. L. Du Toit Memorial Lecture Series* **14**, 32p (1976).
 19. The possibility exists that the inner sheath of a colonial coccoid cyanophyte may have been totally degraded leaving solely the outer sheath preserved. See S. M. Awramik, S. Golubic, E. S. Barghoorn, *Geol. Soc. Am. Abstracts with Programs* **4**, 438 (1972); R. J. Horodyski and S. P. Vonder Haar, *J. Sediment. Petrol.* **45**, 894 (1975); S. Golubic and H. J. Hofmann, *J. Paleontol.* **50**, 1074 (1976).
 20. A. R. Loeblich, *Proc. North Am. Paleontological Convention* (1969), p. 705; *Taxon* **23**, 277 (1974).
 21. Bedding surfaces of the Newland Shales contain carbonaceous films similar to those described and interpreted as megascopic and probably eukaryotic algae from the 1300-million-year-old Greyson Shale, Belt Supergroup, by M. R. Walter, J. H. Oehler, D. Z. Oehler, (5). Such algae, if eukaryotic, could have been the source of the Newland sphaeromorphs. Study of the megascopic films in the Newland shales is in progress.
 22. Studying shale-facies microfossils in petrographic thin sections supplements the study of microfossils in acid maceration residues as it preserves the spatial relationship of the microfossils, avoids breakage of fragile specimens, and indicates whether organic microstructures are indigenous to the rock and syngenetic with deposition of the enclosing sedimentary matrix. In addition, it provides a relatively rapid means of identifying fossiliferous horizons. Interestingly, the microfossils are evident only in petrographic thin sections oriented parallel to bedding; in sections oriented perpendicular to bedding the microfossils are not readily recognizable as biologic entities due to compression.
 23. We thank J. W. Schopf and H. T. Loeblich for discussion.

17 June 1977; revised 19 October 1977

Autoradiographic Image Intensification: Applications in Medical Radiography

Abstract. *The image of an 80 to 90 percent underexposed medical radiograph can be increased to readable density and contrast by autoradiographic image intensification. The technique consists of combining the image silver of the radiograph with a radioactive compound, thiourea labeled with sulfur-35, and then making an autoradiograph from the activated negative.*

Minimizing the x-ray dose received by patients during medical examinations and maximizing the quality of the radiographs are subjects of current concern to both the medical profession and the public (1). Some conflict is inherent in the two objectives because higher-quality radiographs—that is, those which convey more information to the physician—usually require higher exposure levels. Recent gains in quality or exposure reduction, or both, are due to developments such as computer processing, electrostatic imaging systems, improvements in intensifying screens, and scatter rejection techniques (2). The experiments reported here indicate that additional exposure reductions or quality increases are possible with postdevelopment

autoradiographic image intensification.

Radiographs which are normally classified as “badly underexposed” actually contain most of the information which was intended to be recorded by the original exposure. Autoradiographic intensification effectively retrieves this information by increasing the image density and contrast to readable levels. The intensification occurs on an autoradiograph made from the underexposed film after the original image silver has been chemically combined with a radioactive isotope (3). While the theory of autoradiographic intensification has been known for many years (4), the possibility of its widespread application has recently been realized through the development at the Marshall Space Flight Center

of a simple, efficient radiochemical technique employing thiourea labeled with sulfur-35 (5). Although the procedure was developed for use in astronomical research, some of the most valuable applications may be in the field of medical radiography (6). These include reduction of the x-ray dose, since underexposed radiographs can be intensified after development; elimination of retakes necessitated by accidental underexposure; and maximum use of exposures with a high detective quantum efficiency (DQE), such as those made with scatter rejection devices, which can cause underexposures (2, 7).

With the cooperation of scientists from Vanderbilt University Hospital, we determined the range of underexposures which can be adequately intensified by autoradiography. We found that, in general, radiographs underexposed by as much as 80 to 90 percent produce autoradiographs which compare favorably with optimum exposures. Some of the radiographs used for this research were inadvertently underexposed in routine clinical situations, and others were deliberately underexposed.

The underexposure limit for a commonly used film-screen system, DuPont Lo-Dose (single-coated film), was determined from experiments with radiographs of the abdominal area of an anatomical phantom. An optimum-exposure radiograph was made at 120 kV and 450 mA-sec. Underexposures were made (with no change in tube voltage or subject distance) at 100, 50, and 20 mA-sec (that is, underexposures of 78, 89, and 96 percent). Autoradiographs of the underexposed film were made and compared with the normal-exposure radiograph. The contrast and visible detail on the autoradiographs made from the 78 and 89 percent underexposures were about the same as on the normal radiograph. Figure 1 shows optimum paper prints (8) of the normal exposure radiograph, the 89 percent underexposure radiograph, and the autoradiograph of the 89 percent underexposure. The limiting case was the 96 percent underexposure; there was absolutely no visible image on the radiograph, and while the autoradiograph produced an image, it was of unacceptably poor quality. An example of accidental underexposure with the same film-screen system is shown in Fig. 2, where an underexposed mammogram may be compared with the corresponding autoradiograph. All autoradiographs were made on Kodak industrial films with exposure times of 2 to 12 hours (9).

The method of radioactivating radio-